Molecular Crystals and Liquid Crystals Science and Technology. Section A. Molecular Crystals and Liquid Crystals

Publication details, including instructions for authors and subscription information:
http://www.tandfonline.com/loi/gmcl19

Nonlinear Optical Phenomena in the Chiral Smectic A Phase

D. Hermann [a b], L. Komitov [a] & F. Simoni [c]

[a] Department of Physics, Chalmers University of Technology, S-412 96, Göteborg, Sweden

[b] Dipartimento di Scienze Fisiche, Universita degli Studi di Napoli "Federico II", Piazzale V. Tecchio 80, I-80125, Napoli, Italy

[c] Dipartimento di Scienze dei Materiali e della Terra, Università di Ancona, Via Brecce Bianche, I-60131, Ancona, Italy

Version of record first published: 24 Sep 2006.

To cite this article: D. Hermann , L. Komitov & F. Simoni (1996): Nonlinear Optical Phenomena in the Chiral Smectic A Phase, Molecular Crystals and Liquid Crystals Science and Technology. Section A. Molecular Crystals and Liquid Crystals, 282:1, 67-89

To link to this article: http://dx.doi.org/10.1080/10587259608037569

Mol. Cryst. Liq. Cryst., 1996, Vol. 282, pp. 67–89
Reprints available directly from the publisher
Photocopying permitted by license only

Nonlinear Optical Phenomena in the Chiral Smectic A Phase

D. Hermann*, L. Komitov
Department of Physics, Chalmers University of Technology, S-412 96, Göteborg, Sweden

*) Also: *Dipartimento di Scienze Fisiche, Università degli Studi di Napoli "Federico II", Piazzale V. Tecchio 80, I-80125 Napoli, Italy*

F. Simoni
Dipartimento di Scienze dei Materiali e della Terra, Università di Ancona, Via Brecce Bianche, I-60131 Ancona, Italy

Abstract We report a detailed account of a pump-probe experiment on nonlinear optical phenomena in the chiral smectic A phase: opto-thermally induced director reorientation through the electroclinic effect; an optic axis rotation effect; a thermal indexing effect. In particular, we evaluate explicitly the temperature rise due to laser heating as well as the nonlinear phase shift due to the thermal indexing effect. We also show how a modeling of the interplay between the phenomena accounts well for the experimental results. Finally, we discuss the physical origin of the optic axis rotation effect.

1. Introduction

Only few studies on nonlinear optical phenomena in smectics involving reorientation of the director can be found in the literature, contrary to the case of nematic liquid crystals. In 1981, Tabiryan and Zel'dovich [1] studied theoretically the possibility for laser-induced director reorientation in smectics C and smectics A. In 1983, Lippel and Young [2] reported the observation of a purely optically induced reorientation effect in a freely suspended smectic C-film, and a detailed theory of such a phenomenon was presented the same year by Ong and Young [3]. In 1992 a laser-induced reorientation of the director in the chiral smectic-C phase (SmC*) was reported by MacDonald et al. [4] together with a Landau theory and a heat-flow equation accounting for the effect in terms of laser heating of the sample.

In 1995 a laser-induced reorientation of the director in the chiral smectic-A phase (SmA*) due to the electroclinic effect was reported by us [5]. In addition to this effect, we also reported on an optic axis rotation effect of unknown origin, as well as a thermal indexing effect [5]. In the present paper we give a much more detailed and quantitative description of the experiment and the effects, which were only briefly reported in ref. [5].

2. Experimental

2.1. The Sample

The liquid crystal was a ferroelectric mixture from the Chisso Corporation, Japan, called "CL-C100". It is especially designed to exhibit a large electroclinic effect at room temperature. The phase transition sequence is:

SmC* 20°C SmA* 65°C isotropic.

The experimental cell was a sandwich cell consisting of two parallel glass plates with the liquid crystal material in between them. It was oriented in book-shelf geometry [6]; i.e., the smectic layers were perpendicular to the bounding glass plates which imposed planar boundary conditions on the liquid crystal molecules. The glass plates were unidirectionally rubbed on their inner surfaces, and the cell thickness was kept at 2 μm by evaporated SiO_x spacers - thus giving a homogeneous order in the sample. It was necessary to slowly cool the experimental cell after filling it with the liquid crystal in the isotropic phase, in order to keep the bookshelf alignment. The glass plates were coated with transparent, conducting tin oxide-electrodes.

2.2. The Pump-Probe Experimental Setup

The experiment was a pump-probe experiment, set-up as outlined in ref. [7]. The experimental setup is shown in Fig. 1, together with a coordinate system for the laboratory frame.

A strong pump beam from an Ar^+-laser operating at 514.5 nm wavelength, traveling in the $(-x)$-direction and with linear polarization in the y-direction, induced nonlinear optical effects in the liquid crystal cell. The polarization changes arising from these effects were monitored by a weak probe beam from a He-Ne laser at 632.8 nm wavelength, traveling in the $(+x)$-direction. Crossed polarizers were placed before and after the sample in the path of the probe beam. The probe beam was deflected 45° by a beam-splitter, in order to be detected by a photodiode detector. The probe beam was chopped, and amplified by a lock-in amplifier in order to increase the sensitivity of the experiment. Red filters only letting through the probe beam wavelength, were inserted into the path of the probe beam in order to protect the polarizer and analyzer from being burned by the pump beam. Polarizer, analyzer and sample were mounted on angular turntables, permitting rotation through a definite number of degrees of these. Finally, a $\lambda/4$-plate was inserted directly after the aperture of the He-Ne laser, in order to obtain a circularly polarized probe beam. Thus, the polarization plane of the probe beam could be freely turned by the polarizer, P.

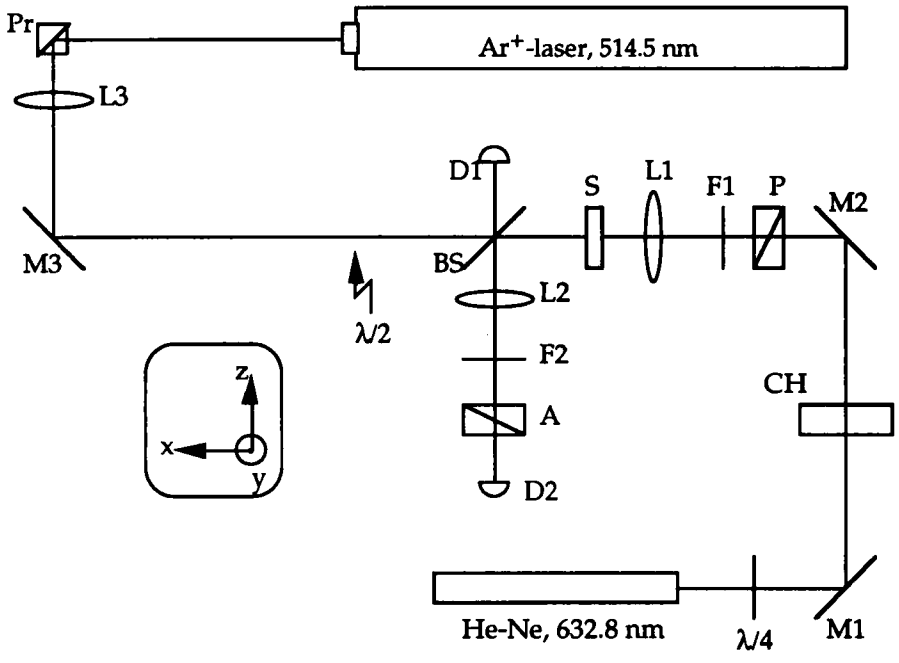

Figure 1: The Experimental Setup for Pump-Probe measurements. **L1:** Lens, $f = 50$ mm (focus probe beam on sample). **L2:** Lens, $f = 100$ mm (focus probe beam on detector D2). **L3:** Lens, $f = 1$ m (loose focus of pump beam on sample). **CH:** Chopper for probe beam (550 Hz). **M1, M2, M3:** Mirrors. **P:** Polarizer for probe beam, mounted on angular turntable. **A:** Analyzer for probe beam, mounted on angular turntable. **F1, F2:** Red filters blocking the pump beam, thus protecting P and A. **S:** Sample, mounted on angular turntable. **BS:** Beam splitter (an object glass for microscopes). **D1:** Spectra Physics power detector for pump power. Calibrated. **D2:** Photodiode detector for probe signal. Lock-In amplified. **Pr:** Nicol Prism, enhancing the pump polarization in the y-direction. $\lambda/4$: For circularly polarized initial probe beam. $\lambda/2$: Insertable. For turning polarization of pump beam through 90°.

2.3. The Experimental Geometry

When an electric field **E** is applied across a sandwich cell where the liquid crystal is in its SmA* phase and aligned in bookshelf geometry, a tilt angle of the molecules is induced in the plane perpendicular to the field and whose magnitude is proportional to the electric field strength:

$$\theta_{ind}(T,E) = e_C(T) \cdot E$$

This is the *electroclinic effect* [8], and $e_C(T)$ is the temperature dependent electroclinic coefficient.

To perform the measurements, the sample was set in different angular positions, depending on the electric field strength applied across the sample. With the field applied, the sample was turned into the angular setting depicted in Fig. 2. One of the extreme switching positions was thus parallel to the polarizer: this state was called "Dark state" - the other, then, was called "Bright state". θ_{ind} in Fig. 2 denotes the electroclinically

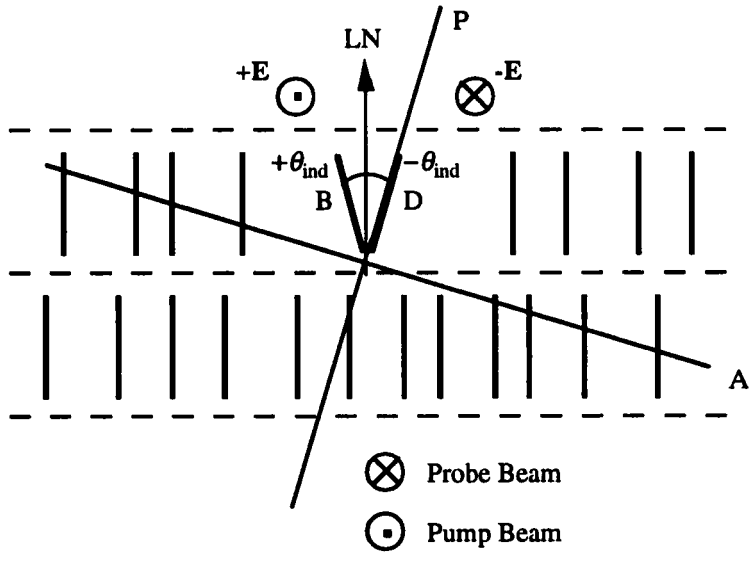

Figure 2: The experimental geometry. LN=Smectic Layer Normal. E=Applied electric field. P=Polarizer. A=Analyzer. B=Bright state. D=Dark state.

induced tilt angle of the molecules. At zero electric field the tilt angle is zero and the Dark and Bright states are degenerate - this is indicated in Fig. 2 by the liquid crystal molecules which are perpendicular to the smectic layers. In this case the sample was turned so that these degenerate states coincided with the polarizer P.

2.4. Transmission Measurements

2.4.1. The Principles of the Measurements

The Pump-Probe arrangement offers the possibility to monitor reorientations of the director, or the optic axis, with a high sensitivity, by detecting the polarization changes of

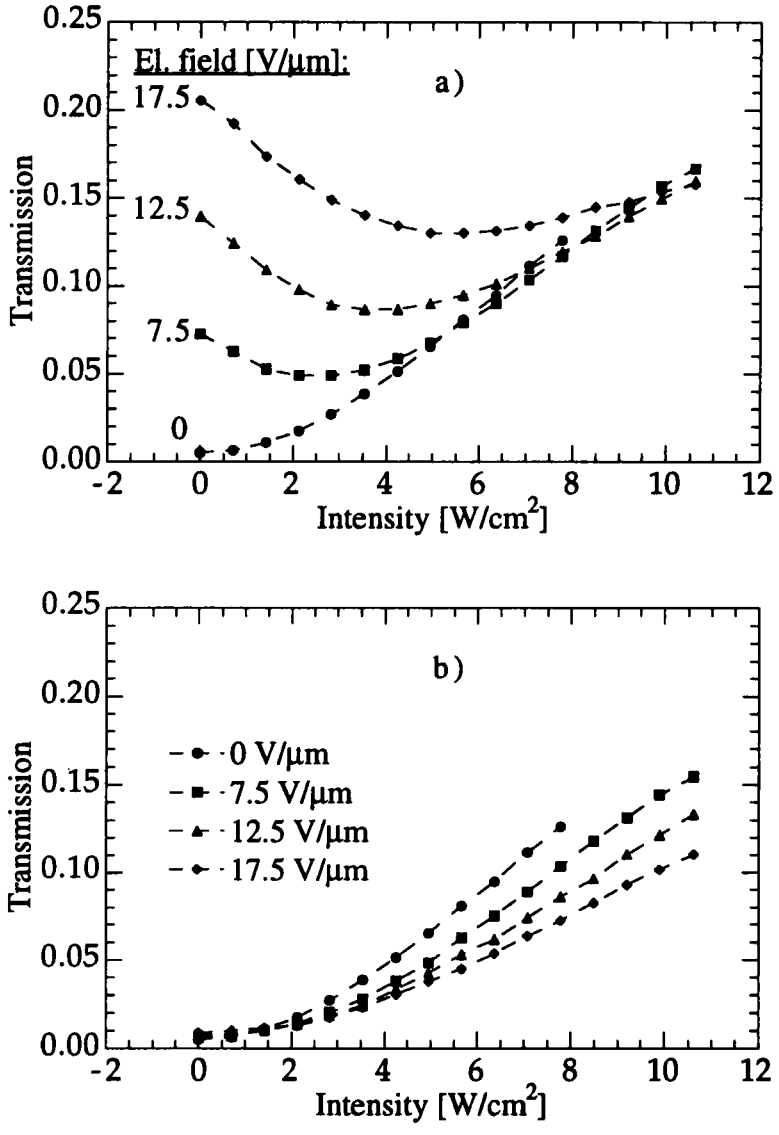

Figure 3: The transmission of the probe beam between crossed polarizers as a function of pump beam intensity and applied electric field strength. *a)* Bright states. *b)* Dark states.

the probe beam. Crossed polarizers (P and A in Fig. 1) are placed before and after the sample in the path of the probe beam, so that these polarization changes manifest themselves as changes in transmission of the light according to [8]:

$$T_{\perp} = \frac{I_{\perp}}{I_0} = \sin^2\left\{\frac{\delta}{2}\right\}\sin^2\{2\phi\} \qquad (1a),$$

where ϕ is the angle between the director (the optic axis) and the polarizer, and δ is the phase shift: $\delta = 2\pi d\Delta n/\lambda$ in standard notation. I_0 is the transmitted intensity through the sample when the polarizers are parallel *and* when $\phi = 0,\ \pi/2,\ \pi,\ 3\pi/2,\ \ldots\ldots$. For parallel polarizers we have [8]:

$$T_{\parallel} = \frac{I_{\parallel}}{I_0} = 1 - \sin^2\left\{\frac{\delta}{2}\right\}\sin^2\{2\phi\} \qquad (1b),$$

and so it is evident from Eq. (1b) that we have $I_0 = I_{\parallel}\left(\phi = 0,\ \pi/2,\ \pi,\ 3\pi/2,\ \ldots\ldots\right)$. This has been used to measure I_0 in each case, simply by setting the analyzer parallel to the polarizer and making sure that also the optic axis was parallel to the polarizers (i.e., that $\phi = 0,\ \pi/2,\ \pi,\ 3\pi/2,\ \ldots\ldots$.

2.4.2. The Measurement Procedure

After the sample had been set to its initial angular position according to Section 2.3. or Fig. 2 above, a series of measurements of the transmission of the probe beam as function of pump laser intensity was performed. The results are shown in Figs. 3a-b for the Bright and Dark states, respectively. Notably there is a transmission change even if $E \equiv |\mathbf{E}| = 0$.

The applied electric field was a square-wave of very low frequency (~0.1-0.2 Hz), in order to have the time to measure the Bright and the Dark states separately.

2.4.3. The Polarization of the Pump Beam

The polarization of the pump beam was turned 90° from the y-direction into the z-direction by means of the insertable $\lambda/2$-plate. No difference in transmission data was found. This indicates that a direct optical reorientation does not occur.

2.5. The Electroclinic Effect

2.5.1. Opto-Thermally Induced Director Reorientation

On illuminating the sample with the pump laser beam, some of the energy that it carries is absorbed by the cell in the point of impingement. This energy absorption mainly takes place in the electrodes of the bounding glass plates of the cell (ref. [4]), and thus causes a partial heating of the sample.

An applied electric field induces a tilt angle as well as a ferroelectric polarization in the SmA*-phase which are sensitive to temperature changes through the temperature dependence of the electroclinic effect. We therefore expect, and find, a decrease of these quantities when increasing the pump intensity.

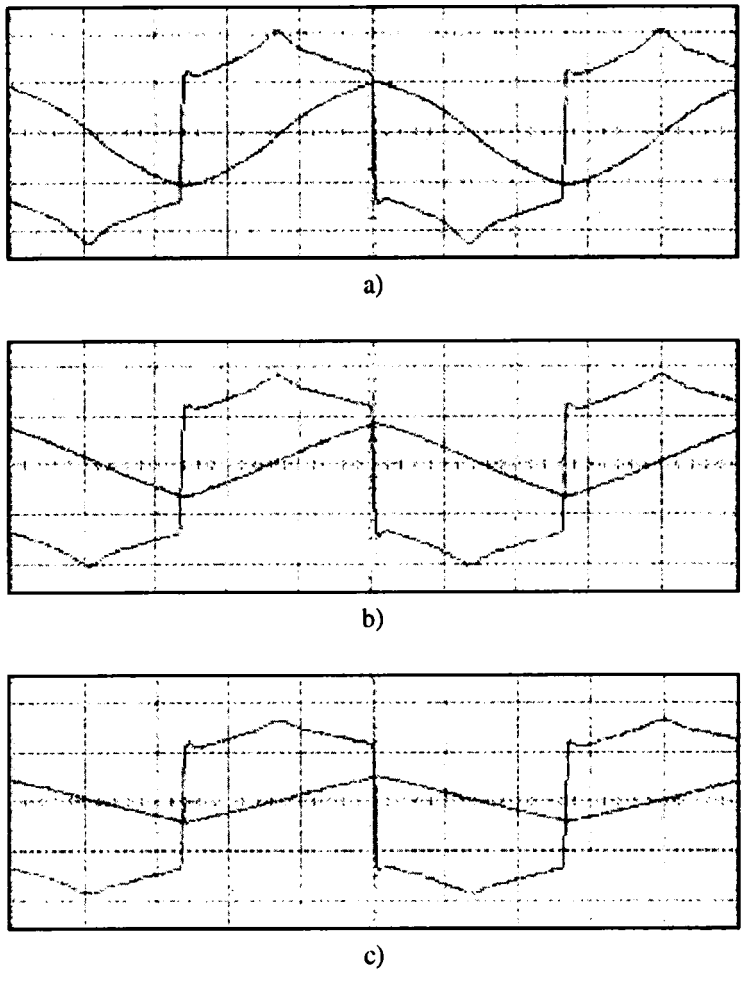

Figure 4: The current (square-like with peaks) and optical (triangle-like) responses on application of a pure triangle-wave (not shown) for different pump intensities: *a)* 0 W/cm^2, *b)* 3 W/cm^2, and *c)* 6 W/cm^2.

In Figs. 4a-c are shown the optical and current responses of the sample for three different pump intensities, on an applied electric field of triangular waveform. Without any pump intensity it is clearly seen how the motion of the liquid crystal molecules with the changes in time of the electric field is a mixture of the cone motion typical of the SmC*-phase and

the in-plane motion of the SmA*-phase [10]. The fast part of the optical response corresponds to the cone motion, which is what gives rise to a reversal of the ferroelectric polarization; the fast part of the optical response is seen to correspond in time with the polarization reversal current peak of the electric response of the cell.

On applying some pump intensity it is clearly seen how the optical response gets a simple, triangular wave form, indicating a pure electroclinic, in-plane switching of the molecules which follow the electric field proportionally. It is also clearly seen how the amplitude of the optical response decreases. This corresponds to the expected decrease of the induced tilt angle of the SmA*-phase with the temperature. Therefore, this effect can be called *opto-thermally induced director reorientation*, as was also found in ref. [4] for the case of the spontaneous tilt angle of the SmC*-phase.

Finally, it can be noted in Figs. 4a-c that the polarization reversal current peak of the electric response decreases, as expected, but that it does *not* disappear. This would apparently contradict the optical response, which indicates that no cone motion takes place. However, there is no contradiction, which can be easily realized: The optical response is measured by the probe beam, and thus probes only the very small area of the liquid crystal cell which is heated by the pump beam. In this point it is true that there is no cone motion. The electric response is on the other hand taken from the electrodes, which means that it is measured over a much bigger area. The entire cell is not heated nearly as much as in the point of impingement of the pump beam, and thus it is also true that cone motion still takes place in the rest of the cell.

2.5.2. The Induced Tilt Angle and The Electroclinic Coefficient

The induced tilt angle θ_{ind} was explicitly measured by an indirect method [11], as a function of pump intensity for several different electric field strengths. See Fig. 5a. The electroclinic coefficient e_C was calculated from the tilt angle measurements through $e_C(I) = \theta_{ind}(I,E)/E$ for each E. The result is shown in Fig. 5b.

Assuming a temperature rise δT proportional to the pump intensity [12] ($\delta T = kI$) the expression for $e_C(T)$ [13] was adapted to laser heating:

$$e_C(I) = \frac{\mu}{\alpha(\Delta T + kI)^{\gamma} - \frac{\mu^2}{\varepsilon}} \quad ; \quad \Delta T \equiv T_{ambient} - T_C \qquad (2),$$

where μ is the structural coefficient (basically the bilinear coupling constant between the molecular tilt angle and the ferroelectric polarization), ε is the high temperature dielectric permittivity of the SmA*-phase and $\alpha\Delta T$ is the first coefficient of the Landau free energy expansion for a liquid crystal. The critical exponent γ has also been included, for generality. A curve fit of Eq. (2) was made to the data for e_C. The fit parameters are

given in Table 1. From Table 1 the constant k in $\delta T = kI$ can be determined, knowing that $\Delta T \approx (8-9)$ K: $k = (0.47-0.53)$ K cm^2/W.

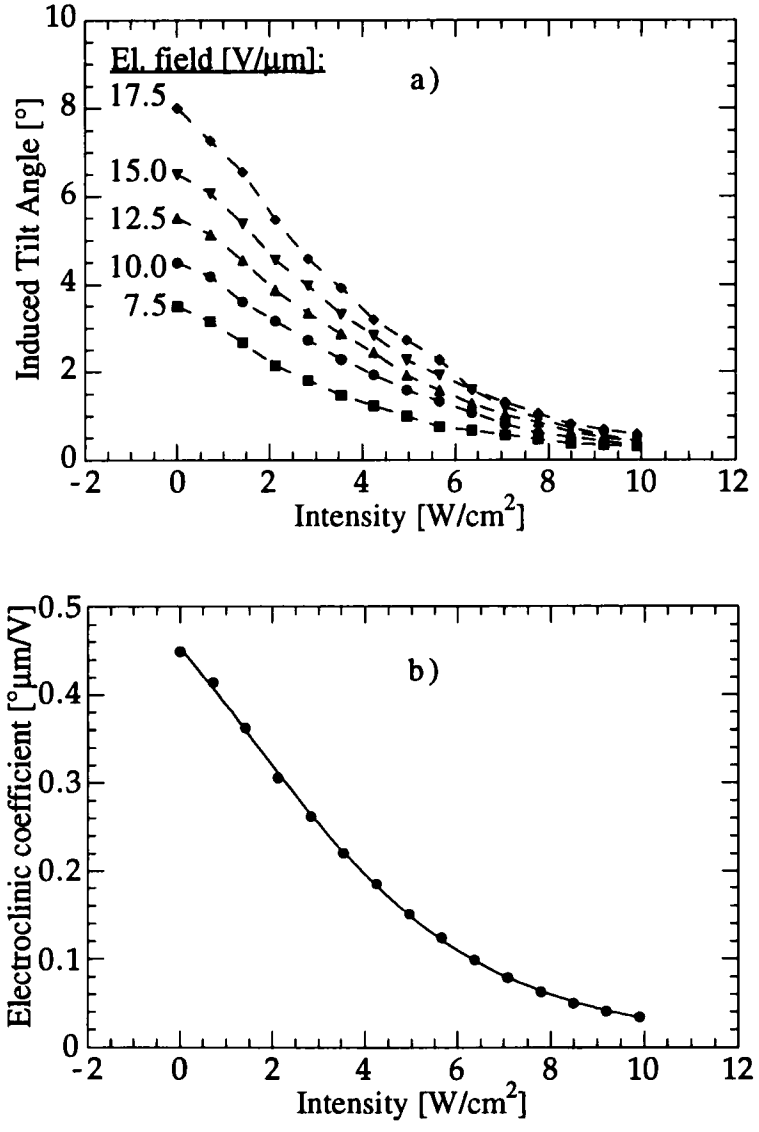

Figure 5: *a)* The induced tilt angle as function of pump beam intensity for different electric field strengths. The dashed lines connect the data points for clarity. *b)* The electroclinic coefficient, calculated from the tilt angles. The solid line shows a curve fit according to Eq. (2) and Table 1.

Fit parameter	Value	Error
$\frac{\mu}{\alpha k^7}$	$3.5970 \cdot 10^{10}$	$6.2101 \cdot 10^{10}$
$\frac{\Delta T}{k}\left[\mathrm{W/cm^2}\right]$	17.044	3.254
γ	8.39	1.15
$-\frac{\mu}{\alpha k^7} \cdot \frac{\mu}{\varepsilon}$	$5.7871 \cdot 10^{10}$	$9.8175 \cdot 10^{10}$
χ^2	$1.1776 \cdot 10^{-4}$	-
R	0.99979	-

Table 1: The electroclinic fit parameters.

2.6. The Optic Axis Rotation Effect

The non-zero transmission at $E = 0$ found in Fig. 3a-b, and the initial condition $\phi = 0°$ imply that there must be a change in the optic axis direction ϕ when the pump intensity is increased. Such a change in ϕ was indeed discovered, and measured explicitly as a function of pump intensity. Each time the pump intensity was increased the probe transmission increased. The sample was turned around the x-axis until a minimum in transmission again was found. The magnitudes of each turn were recorded and added together. In this manner the total deviation of the optic axis was measured as a function of pump intensity. See Fig. 6. The effect was found to be reversible, and the measurement could be repeated several times.

The data exhibit an almost linear relationship with laser intensity. Therefore, the following equation, satisfying the constraint that $\psi(0) = 0°$, was used to fit the data:

$$\psi(I) = aI \tag{3}.$$

The results are given in Table 2.

A test on the nature of the optic axis rotation effect was also made: instead of using the pump laser beam, the sample was uniformly heated by means of a hot-air blower while the transmission of the probe beam was checked. There was no change, however, in the transmission, indicating that the optic axis rotation effect either is a purely optical interaction between the radiation field and the liquid crystal, or that it is a thermal effect which can only be induced by temperature gradients due to the local heating by the pump beam.

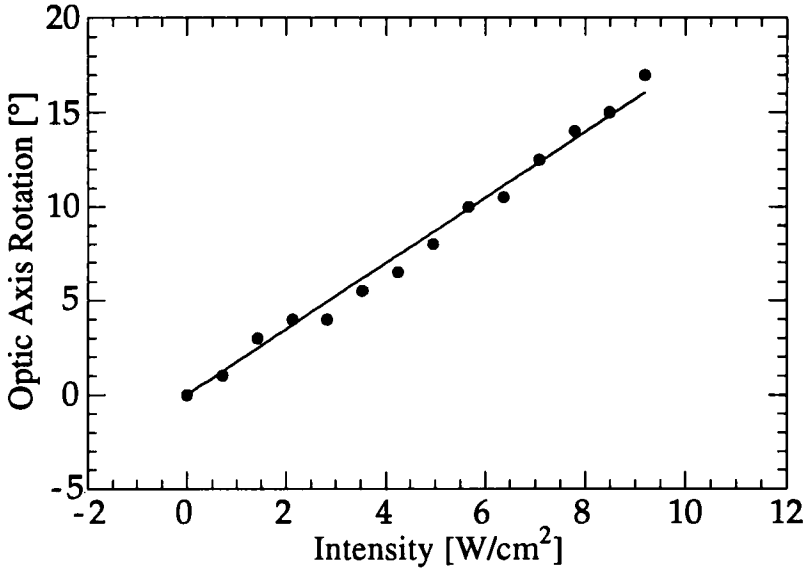

Figure 6: The optic axis rotation as function of pump beam intensity. No electric field is applied. The solid line shows a curve fit according to Eq. (3) and Table 2.

Fit parameter	Value	Error
$a \left[\frac{\text{deg cm}^2}{\text{W}}\right]$	1.7469	0.029125
χ^2	4.5189	-
R	0.99396	-

Table 2: Fit parameter for the optic axis rotation effect.

2.7. Phase Shift and Birefringence of the Sample

The sample was placed between crossed polarizers in a separate setup with a He-Ne laser and a power meter as detector. The phase shift δ and the birefringence Δn were measured by simply turning the sample through 360° around the direction of the He-Ne laser beam while monitoring the transmission of the beam. The result is shown in Fig. 7. The amplitude M, indicated by the dotted line in Fig. 7, was measured directly from the figure as the average value of the magnitudes of the four

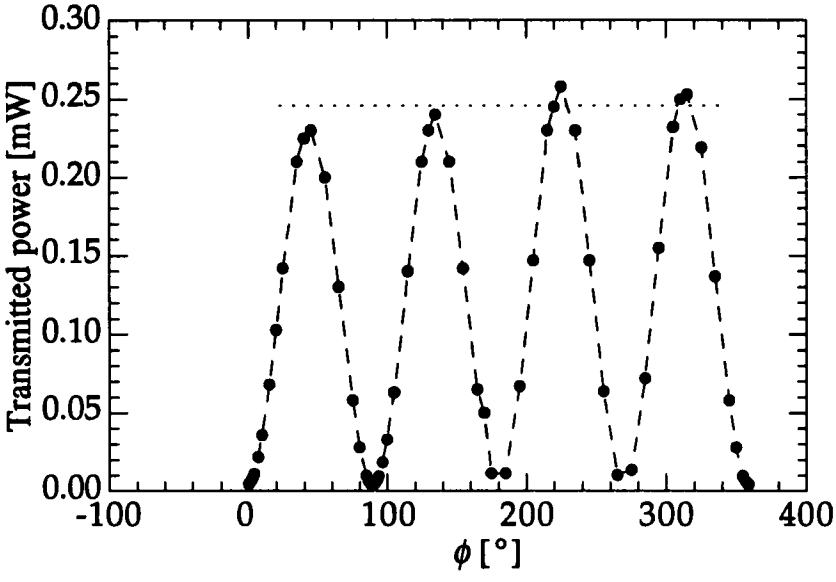

Figure 7: Measurement of the phase shift or birefringence of the sample when *no* pump beam radiation and *no* electric field is applied. The sample between crossed polarizers is turned through 360°. The light source is a low power He-Ne laser.

slightly different maxima in the figure. The maximum intensity for parallel polarizers, I_0, was measured according to Section 2.4.1. From Eq. (1a) we have:

$$I_\perp = \left[I_0 \sin^2 \frac{\delta}{2}\right] \cdot \sin^2\{2\phi\} \quad ; \quad M = I_0 \sin^2 \frac{\delta}{2}$$
$$\Downarrow \qquad (4).$$
$$\delta = 2 \arcsin \sqrt{\frac{M}{I_0}}$$

With $M = 0.245$ mW and $I_0 = 0.260$ mW we get directly from Eq. (4) the phase shift of the sample to be $\delta = 152°$. From this we directly get the birefringence as well:

$$\Delta n = \frac{\lambda \delta}{2\pi d} = 0.13$$

using $\lambda = 632.8$ nm and $d = 2\ \mu$m. The birefringence is within the expected range for a liquid crystal.

2.8. *Thermal Indexing*

To examine the role of thermal indexing, the transmission measurement at zero electric field could be used together with the information contained in Eq. (3) and in Table 2 about the optic axis rotation effect. Two curves were calculated and compared to the $E = 0$ transmission data: one assuming *no* thermal indexing; the other assuming it:

$$\text{No thermal indexing:} \qquad T = \sin^2\{aI\}\sin^2\left\{\frac{\delta_0}{2}\right\} \tag{5a}$$

$$\text{Thermal indexing:} \qquad T = \sin^2\{aI\}\sin^2\left\{\frac{\delta_0 + \kappa I}{2}\right\} \tag{5b}$$

where in Eq. (5b) a Kerr-type optical nonlinearity has been assumed, giving an intensity dependent phase shift according to:

$$\delta(I) = \delta_0 + \kappa I \tag{6}.$$

In this context, δ_0 is meant to be the value of the phase shift of 152° which was measured independently as described in Section 2.7. The fixed values of a and δ_0 were inserted into Eqs. 5a-b, the transmissions were calculated and plotted together with the

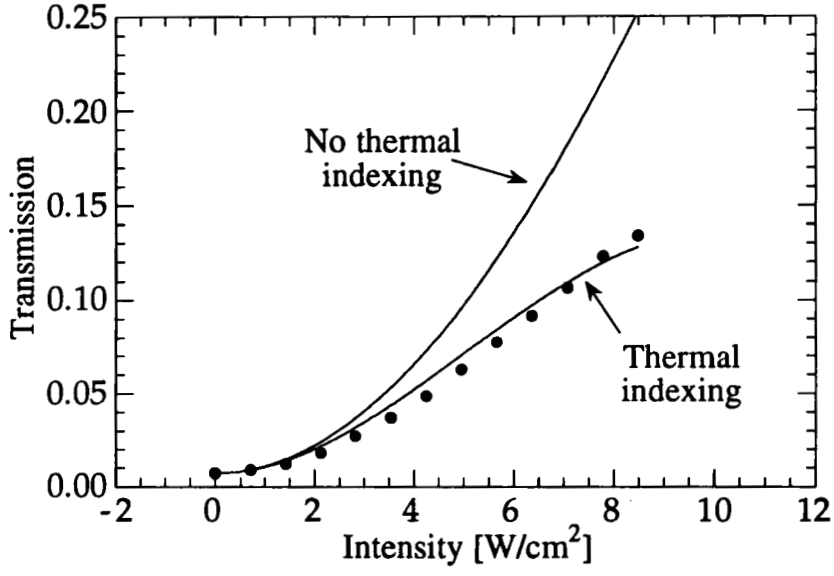

Figure 8: Calculations according to Eqs. (5a-b) of the transmission at zero electric field for the absence and presence of the thermal indexing effect.

experimental data in Fig. 8. In Eq. (6) the nonlinear phase shift parameter κ is unknown, why it was left as a fitting parameter in Eq. (5b). Thus, the plot of Eq. (5b) in Fig. 8 is a curve fit to the experimental data with only one parameter, allowing a determination of the value of κ.

It is clear from Fig. 8 that a nonlinear phase shift $\delta_{NL} = \kappa I$ must be assumed in order to get a more correct description of the transmission data. The fit of Eq. (5b) yields a value of $\kappa \approx -7$ deg cm^2/W. The negative sign suggests that it is thermal indexing which is the mechanism responsible for the nonlinear phase shift.

3. Modeling the Transmission Data

With the different measurements described above it is possible to account for the behavior of the total transmission in Figs. 3a-b, qualitatively and to a great extent quantitatively. To this end a very simple model for how the electroclinic effect and the optic axis rotation effect act together on the overall angle $\phi(I,E)$ between the optic axis and the polarizer was established. An underlying assumption of the model is that the two effects are independent of each other in the sense that when the sample is illuminated with a certain intensity, the optic axis has rotated through a certain angle according to Eq. (3); now, when an electric ac field is applied, the molecules begin to switch according to the electroclinic effect, meaning that they switch *symmetrically* around the particular angular position imposed by the optic axis rotation effect. In fact, this assumption was also tested experimentally by checking the two (electroclinic) switching positions under application of the electric field and the angular position without application of the electric field, for a given pump intensity. In each case, the latter angular position fell precisely in the middle between the two former ones. On these grounds it is assumed that the two effects are independent of each other and that the overall effect can be obtained by simply adding them together.

By inspection of Fig. 3a for the transmission of the Bright states, it is clear that the two effects in this case must *counteract* each other since the curves for $E \neq 0$ have minima. Therefore we can write $\phi(I,E)$ as:

$$\phi(I,E) = \theta_0(E) \pm \theta_{ind}(I,E) - \psi(I) \tag{7}.$$

In Eq. (7) all angles are defined as positive angles. $\theta_0(E)$ denotes the initial setting of the sample in order to make $\phi = 0$ for the Dark state when $I = 0$. The double sign accounts for the Dark (-) and Bright (+) states, respectively. $\theta_{ind}(I,E)$ denotes the tilt angle induced by the electroclinic effect. $\psi(I)$ denotes the optic axis rotation effect, and the negative sign in front of it denotes a counteraction to the Bright state.

Inserting $\theta_0(E) = e_C(0) \cdot E$ for the initial setting, $\theta_{ind}(I,E) = e_C(I) \cdot E$ for the induced tilt angle and Eq. (3) into Eq. (7), and then inserting Eqs. (7) and (6) into Eq. (1a) we obtain the overall expression describing the transmission of the probe beam through the sample:

$$T_{B,D}(I,E) = \sin^2\left\{\frac{\delta_0 + \kappa I}{2}\right\}\sin^2\left\{\left[e_C(0) \pm e_C(I)\right] \cdot E - aI\right\} \quad (8),$$

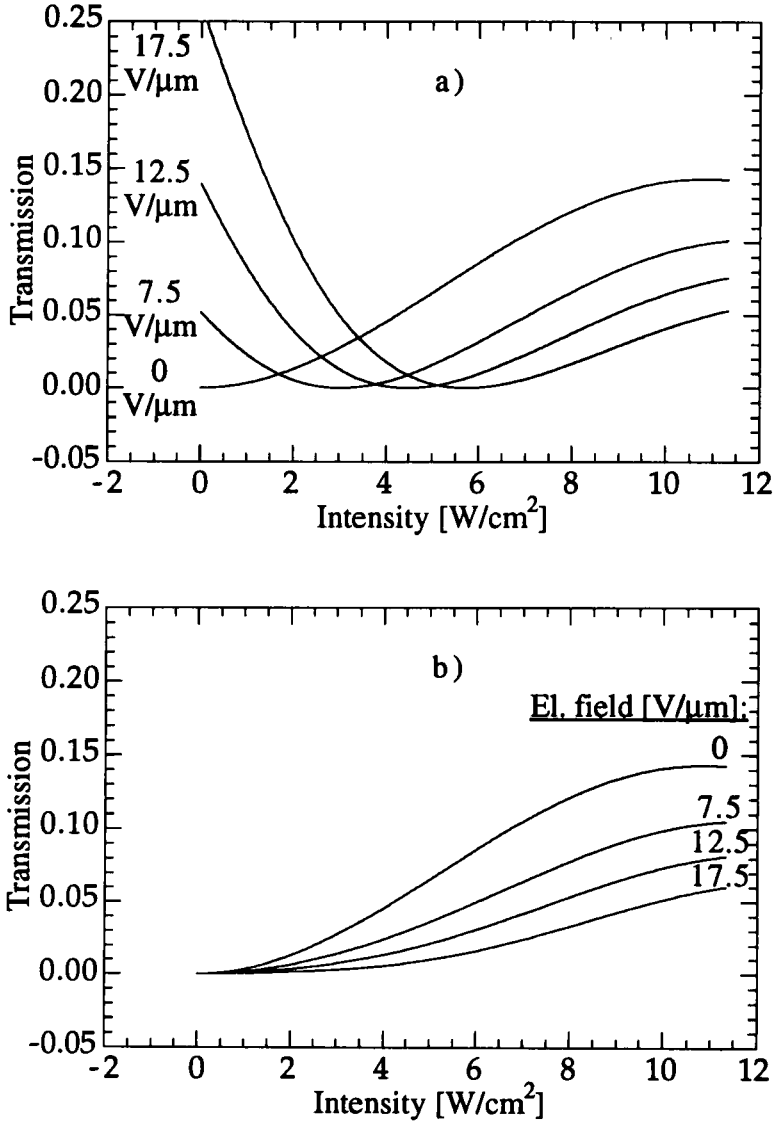

Figure 9: Calculations of the transmission of the probe beam as a function of pump beam intensity and electric field according to Eq. (8), based on the model of Eq. (7).

where e_C is given by Eq. (2). The values of the various fit parameters which are listed in Tables 1 and 2 and those values which were found for δ_0 and κ were inserted into Eq. (8), and the overall transmission curves for the Dark and the Bright states were calculated. These are shown in Figs. 9a-b.

The qualitative features of the calculated curves agree well with those of the measured ones. Note especially that the minima in the curves for the Bright state increase in the x-axis (intensity) position as the applied electric field strength is increased, just as is found experimentally in Fig. 3a. Also, the Dark states have overall a lower transmission when the electric field strength is increased, just as in Fig. 3b.

4. Results and Discussion

To summarize the results of the present experiment, we see that three different effects, when acting together, describe the overall behavior of transmission that was found in Figs. 3a-b: opto-thermally induced director reorientation through the electroclinic effect; an optic axis rotation, causing a deflection of the optic axis which is proportional to the laser intensity; and a decrease of birefringence, suggesting the presence of thermal indexing.

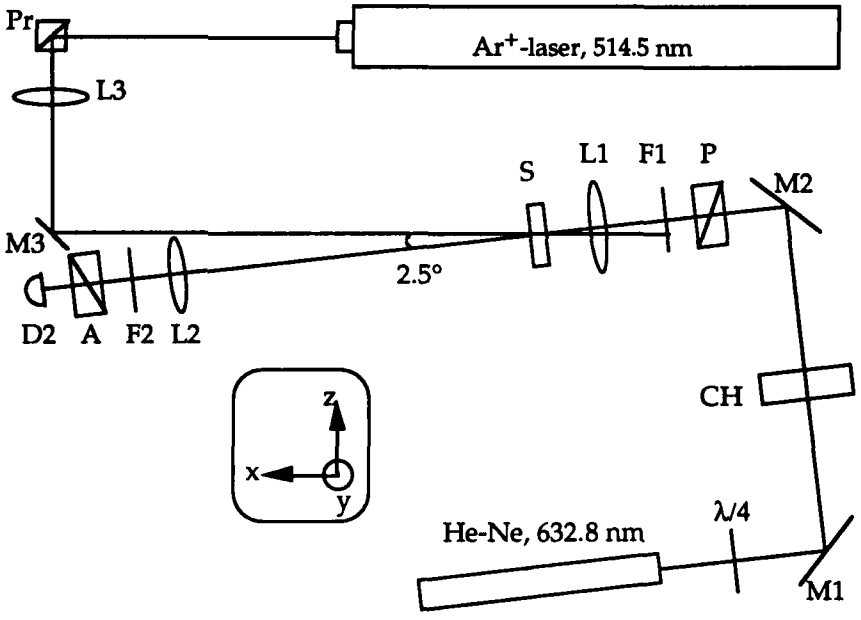

Figure 10: The "straightened" experimental setup. The beam splitter has been removed.

4.1. Calculated versus Measured Transmission Results

Apart from the qualitative features mentioned in Section 3 above that agree between the calculated and the measured transmission curves, it is also clear from Figs. 3a-b and Figs. 9a-b that are some discrepancies, especially for the Bright states. Firstly, the actual intensities for which the minima of the Bright states occur differ between Figs. 3a and 9a. This can probably be attributed to an insufficient accuracy in the values of the fitted parameters, as well as to changes in the degree of book-shelf alignment of the liquid crystal during the course of the experiments. The important point in this case is that in *both* the experimental and the calculated case the intensities for which the minima occur, increase.

Another discrepancy, evident from the Bright state curves in Figs. 3a and 9a, is that the calculated curves reach minima of zero transmission whereas the experimental curves have non-zero minima. This can be attributed to the beam-splitter in the experiment which was an ordinary object glass for microscopes (see Fig. 1), which means that the light emerging behind the sample and impinging on the glass plate is reflected (and transmitted) according to Fresnel's formulae of reflection and transmission of polarized light - in short, the polarization components parallel and perpendicular to the plane of incidence of the glass plate are reflected differently. The consequence is non-zero minima, which was also explicitly checked experimentally: the beam-splitter (glass plate) was removed and the setup "straightened" according to Fig. 10. One transmission measurement was made for the Bright and the Dark state at $E = 12.5\ \mathrm{V}/\mu\mathrm{m}$, shown in Fig. 11a. We now see that the curve for the Bright state indeed reaches zero transmission at the minimum. Moreover, the curve for the Bright state shows a *lower (!)* transmission than the Dark state. Also this is consistent with our model, as shown in Fig. 11b where the calculated curves from Figs. 9a-b for the Bright and Dark state for $E = 12.5\ \mathrm{V}/\mu\mathrm{m}$ are plotted in the same diagram, offering the direct comparison with the results in Fig. 10a. As we can see, our model also reproduces this finding.

4.2. Temperature, Laser Intensity and Consistency with Thermal Indexing

In the following we will show how it is possible to obtain the temperature increase in the point of impingement in the liquid crystal cell as a consequence of a rise in laser intensity; i.e., we will evaluate the quantity dT/dI in three different ways; and at the same time show how this value is consistent with thermal indexing being the mechanism responsible for the nonlinear phase shift described in Eq. (6).

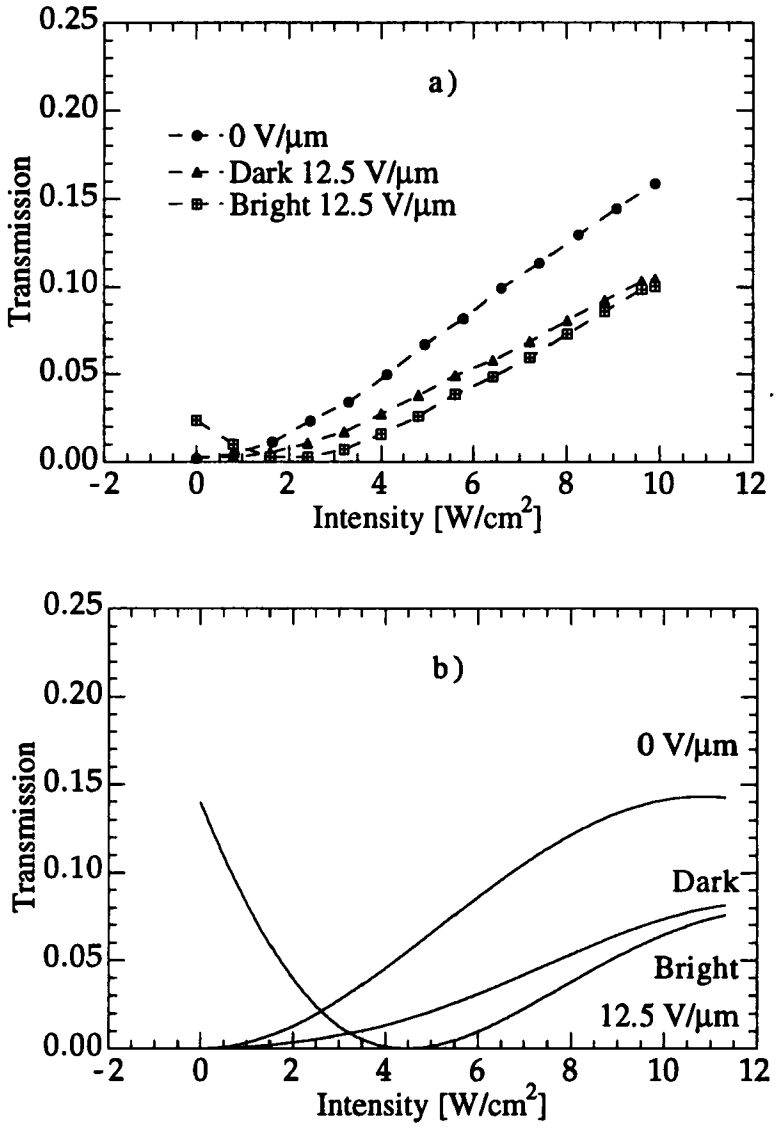

Figure 11: *a)* Measurements of the transmission from the "straightened" setup of Fig. 10. The minimum for the Bright state is now seen to reach zero transmission, just like the calculated curves of Fig. 9a. *b)* The corresponding calculated curves, taken from Figs. 9a-b, for comparison. Notably, the Bright state has a *lower* transmission than the Dark state in both cases.

4.2.1. The Electroclinic Coefficient

In Eq. (2) for the electroclinic coefficient the total temperature was written as

$$T(I) = T_{\text{ambient}} - T_C + kI \tag{9}.$$

Taking the derivative with respect to I we get immediately what we are looking for:

$$\frac{dT}{dI} = k \tag{10}.$$

In Section 2.5.2. the constant k was evaluated, so from the curve fit of the electroclinic coefficient we get directly that

$$\frac{dT}{dI} \approx 0.5 \ \text{Kcm}^2/\text{W} \tag{11}.$$

4.2.2. The Induced Tilt Angle, Temperature and Intensity

The induced tilt angle can be regarded as a function of intensity via its temperature dependence according to Eq. (9) and as a function of electric field strength; i.e., we have:

$$\theta = \theta(T(I), E) \tag{12}.$$

On differentiating we obtain:

$$\frac{\partial\theta}{\partial I} = \frac{\partial\theta}{\partial T} \cdot \frac{dT}{dI} \quad \Rightarrow \quad \frac{dT}{dI} = \frac{\partial\theta/\partial I}{\partial\theta / \partial T} \tag{13}.$$

Previous measurements of the induced tilt angle as a function of electric field strength for several temperatures made it possible to extract a $\theta(T)$-curve which is shown in Fig. 12. From this curve the temperature derivative of the induced tilt angle can be evaluated as shown in Fig. 12, yielding $\partial\theta/\partial T \approx -0.55$ deg/K at $T = 30°\text{C}$ for $E = 5$ V/μm. Proceeding in the same manner the intensity derivative of the induced tilt angle can be evaluated from the corresponding curve in Fig. 5a, the closest electric field strength being $E = 7.5$ V/μm. This yields $\partial\theta/\partial I \approx -0.43$ deg$\cdot$cm^2/W at $I = 3-4$ W/cm^2 Eq. (13) now gives us directly:

$$\frac{dT}{dI} \approx 0.8 \ \text{Kcm}^2/\text{W} \tag{14}.$$

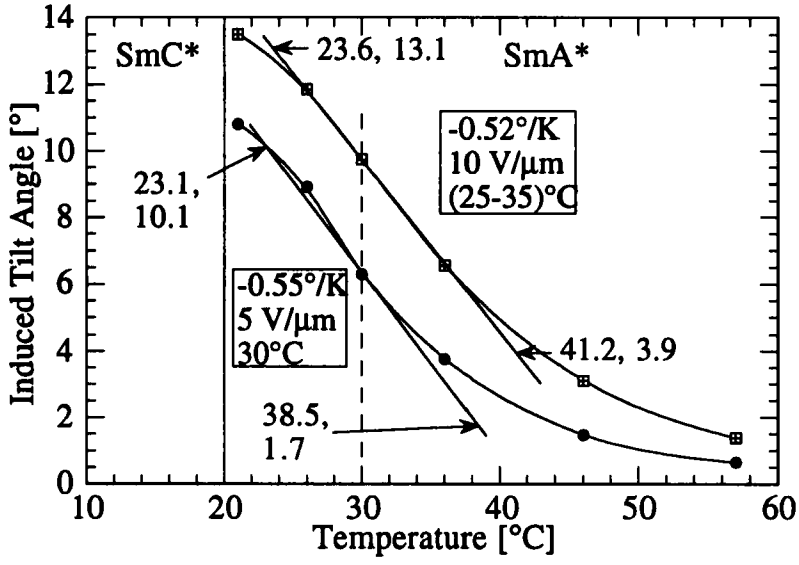

Figure 12: The induced tilt angle as function of temperature for two different electric field strengths. The slopes of the curves are calculated at a temperature corresponding to that of the laboratory.

4.2.3. Nonlinear Birefringence and Thermal Indexing

The birefringence is generally related to the phase shift as

$$\Delta n = \frac{\lambda \delta}{2\pi d} \tag{15}.$$

On differentiating we get:

$$\frac{d[\Delta n(I)]}{dI} = \frac{\lambda}{2\pi d} \cdot \frac{d[\delta(I)]}{dI} \tag{16}.$$

For thermal indexing, the birefringence will be temperature dependent. Applying the chain rule to the left hand side of Eq. (16) in order to get the temperature derivative of the birefringence, and inserting Eq. (6) for the intensity dependent phase shift into the right hand side of Eq. (16), we obtain:

$$\frac{d(\Delta n)}{dT} \cdot \frac{dT}{dI} = \frac{\lambda}{2\pi d} \cdot \kappa \tag{17}.$$

Noting that $\Delta n = n_e - n_o$ and replacing 2π by 360° (since κ in Section 2.8 is given in units involving degrees, not radians) we find what we are looking for:

$$\frac{dT}{dI} = \frac{\lambda\kappa}{d \cdot 360°} \Big/ \left(\frac{dn_e}{dT} - \frac{dn_o}{dT} \right) \tag{18}.$$

For thermal indexing, a typical value for the denominator is $\sim -10^{-2}$ K^{-1}. Inserting this value and $\lambda = 514.5$ nm, $d = 2$ μm and $\kappa = -7$ deg·cm^2/W into Eq. (18) we finally get:

$$\frac{dT}{dI} \sim 0.5 \ \mathrm{Kcm^2/W} \tag{19}.$$

This value corresponds remarkably well with those found in Eqs. (11) and (14). This means that both the order of magnitude of the effect *and* the sign ($\kappa < 0$) is consistent with thermal indexing.

4.3. Origins of the Experimentally Found Effects

It is clear that the director reorientation through the electroclinic effect and the thermal indexing effect that have been found occur due to an increase of temperature in the liquid crystal from some absorption of laser radiation. From Eqs. (9), (11), (14) and (19) we see that the temperature rise was at most 5-8 K, as the highest intensity used in the experiment was about 10 W/cm^2

The physical origin of the optic axis rotation effect is, however, unknown as yet. As mentioned in Section 2.6 this effect could *not* be observed when the sample was uniformly heated, so its origin must be either a purely optical one, or it must be a thermal interaction requiring temperature gradients in the sample induced by the transversal intensity profile of the laser beam. Another important point to note is that the effect is asymmetric, i.e. that there is a deflection of the optic axis in one definite sense. This fact ought to be closely connected with the fact that the smectic liquid crystal consists of *chiral* molecules. The chirality is the element of the system which is sure to be asymmetric, and it is also what gives rise to the electroclinic effect and to the ferroelectric polarization.

Another hypothesis is a rotation of the smectic layers. Normally, smectic layer rotation can be induced by asymmetric ac electric fields [14]. A problem with the hypothesis is whether an optical field could have such an effect. Another problem is that smectic layer rotation is an irreversible process; the observed effect, however, was reversible.

Still another hypothesis which may be made is that of a flow-induced reorientation of the liquid crystal molecules. In this case, the temperature gradient due to the transverse intensity profile of the laser beam would give rise to a flow, supposedly along the smectic layers since each such layer can be regarded as a fluid. This flow in turn would induce a torque, which then would reorient the molecules. Schematically, this could be expressed as:

$$\underset{\text{Temperature gradient}}{\frac{\partial T}{\partial r}} \rightarrow \underset{\text{Flow}}{v_r} \rightarrow \underset{\text{Torque}}{\frac{\partial \mathbf{n}}{\partial \phi}} \rightarrow \underset{\text{Reorientation}}{\Delta\phi}$$

where r denotes a transversal, spatial coordinate along the smectic layers, $\mathbf{n}$ denotes the molecular director and where ϕ denotes the orientation of the director with respect to some reference direction (such as the polarizer). The only problem with this hypothesis is that of symmetry: the temperature gradient is symmetric, and so would cause a flow away from the center of the laser beam, in this case in opposite directions along the smectic layers. Then there would be no net deflection of the effective optic axis of the sample. This could be explained, however, by the asymmetry which is always present in the system due to the chirality of the molecules, e.g. in terms of the surface electroclinic effect [15]. Such an asymmetry, perhaps together with some small geometrical asymmetry of the cell itself (like the glass plates not being perfectly parallel), could cause the liquid crystal to prefer one of the directions in which to flow over the other.

5. Conclusions and Future Work

From the present experiments we can draw the following conclusions:

- A light-induced director reorientation has been observed to take place due to the electroclinic effect.
- A decrease of birefringence has been observed, which is consistent with a thermal indexing effect.
- An optic axis rotation effect, of unknown origin, has been found. It seems to be due to temperature gradients induced by the transversal beam intensity profile, causing a flow-induced torque on the molecular director.
- The maximum temperature rise due to laser heating has been evaluated to be 5-8 K.
- The maximum nonlinear phase shift due to thermal indexing has been evaluated to be about -70°.

It is clearly necessary to clarify the origin of the optic axis rotation effect. Therefore, other liquid crystalline compounds or mixtures with a SmA*-phase must be examined for the presence or absence of the effect. Other experimental techniques are also needed; especially, the simultaneous observation by a polarizing microscope is required, in order to observe possible texture changes during the irradiation by the pump laser beam. These further studies are currently under way.

6. Acknowledgements

D. Hermann acknowledges a research fellowship of Istituto Nazionale di Fisica della Materia (INFM) within the "HUMAN CAPITAL & MOBILITY" program of the European Economic Community, making it possible to carry out this work at the *Dipartimento di Scienze Fisiche, Università degli Studi di Napoli "Federico II", Piazzale V. Tecchio 80, I-80125 Napoli, Italy.* This work has been supported by INFM and the Consiglio Nazionale delle Ricerche (CNR).

A. Maggio, M. Gesini and B. D'Amato at Naples are gratefully acknowledged for technical assistance. G. Andersson at Gothenburg is gratefully acknowledged for providing the data from which Fig. 12 could be drawn.

7. References

[1] N. V. Tabiryan and B Ya. Zel'dovich, *Mol. Cryst. Liq. Cryst.* **69**, 31 (1981).
[2] P. H. Lippel and C. Y. Young, *Appl. Phys. Lett.* **43**, 909 (1983).
[3] H. L. Ong and C. Y. Young, *Phys. Rev. A*, **29**, 297 (1983).
[4] R. MacDonald, J. Schwartz and H. J. Eichler, *Int. J. Nonlinear Opt. Phys.* **1**, 103 (1992).
[5] D. Hermann, L. Komitov and F. Simoni, *Opt. Lett.* **20**, 1116 (1995).
[6] N. A. Clark and S. T. Lagerwall, *Appl. Phys. Lett.* **36**, 899 (1980).
[7] C. Umeton, A. Sgrò and F. Simoni, *J. Opt. Soc. Am. B*, **4**, 1938 (1987).
[8] S. Garoff and R. B. Meyer, *Phys. Rev. Letters*, **38**, 848 (1977) and *Phys. Rev. A*, **19**, 338 (1979).
[9] M. Born and E. Wolf, *Principles of Optics*, Pergamon Press, ed. 5 (1975).
[10] G Andersson, I. Dahl, W. Kuczynski, S. T. Lagerwall, K. Skarp and B. Stebler, *Ferroelectrics*, **84**, 285 (1988).
[11] G. Andersson, I. Dahl, L. Komitov, S. T. Lagerwall, K. Skarp and B. Stebler, *J. Appl. Phys.* **66**, 4983 (1989).
[12] F. Simoni, in *Nonlinear Optical Phenomena in Nematics*, in Physics of Liquid Crystalline Materials, ed. by I. C. Khoo and F. Simoni (Gordon and Breach Science Publishers, New York, 1991), pp. 365-394.
[13] F. Gouda, G. Andersson, S. T. Lagerwall, K. Skarp, B. Stebler, T. Carlsson, B. Zeks, C. Filipic and A. Levstik, *Liq. Cryst.* **6**, 219 (1989).
[14] G. Andersson, I. Dahl, L. Komitov, S. T. Lagerwall, M. Matuszczyk and K. Skarp, poster at 13th ILCC, Vancouver, Canada (1990).
[15] J. Xue and N. Clark, *Phys. Rev. Lett.* **64**, 307 (1990).